Tungsten-Surface-Structure Dependence of Sputtering Yield for a Noble Gas*)

Hiroaki NAKAMURA[1,2], Seiki SAITO[3], Atsushi M. ITO[1] and Arimichi TAKAYAMA[1]

[1]*National Institute for Fusion Science, Toki, Gifu 509-5292, Japan*

[2]*Nagoya University, Toki, Gifu 509-5292, Japan*

[3]*National Institute of Technology, Kushiro College, Kushiro, Hokkaido 084-0916, Japan*

(Received 27 November 2015 / Accepted 7 April 2016)

Using the binary-collision approximation simulation with atomic collision in any structured target code AC∀T, we calculated sputtering yield, range, and retention rate for tungsten with a rough surface under argon atom irradiation. The simulation revealed the sputtering yield decreases and the retention rate increases as the surface becomes rougher. Because these quantities strongly depend on the surface, we suggest that it is necessary to consider the surface structure of the tungsten target when estimating the effects of walls.

Keywords: binary collision approximation, sputtering yield, fuzz structure, tungsten, argon, irradiation, range, retention rate, surface structure

DOI: 10.1585/pfr.11.2401080

1. Introduction

Tungsten nanostructure [1–6] is a phenomenon that has attracted attention in fusion science. Under helium plasma irradiation, a "bubble" structure is formed around the surface of tungsten [1,2]. For the special case when the tungsten temperature is 1000 - 2000 K and the incident energy of the helium plasma is 20 - 100 eV, a nanofilament structure, called a "fuzz" structure, is generated on the tungsten surface [3, 4]. To explain these experimental results, theories [7–9] of the formation of the fuzz structure have been proposed. We reproduced [8, 9] the fuzz structure in a hybrid simulation combining molecular dynamics and Monte-Carlo methods.

Nishijima *et al.* measured [10] the sputtering yields of He-induced W fuzz surfaces bombarded by Ar. According to their results, the sputtering yield of the fuzz surface decreases with increasing fuzz layer thickness L. They suggested [10] that the cause of the reduction in sputtering yield with fuzz could be the direct line-of-sight deposition of sputtered W atoms onto neighboring fuzz before being ejected into the plasma. In this study, we investigate the reliability of their analysis using a binary collision approximation (BCA) [11–15]. The BCA simulation is performed by the atomic collision in any structured target (AC∀T) code [16–19].

The fuzz structure has a complicated shape; therefore, we modeled it as a simple structure (see Fig. 1). Performing the AC∀T simulation for a simplified fuzz structure, we investigated the fuzz layer thickness L dependence of the sputtering yield for Ar irradiation onto tungsten.

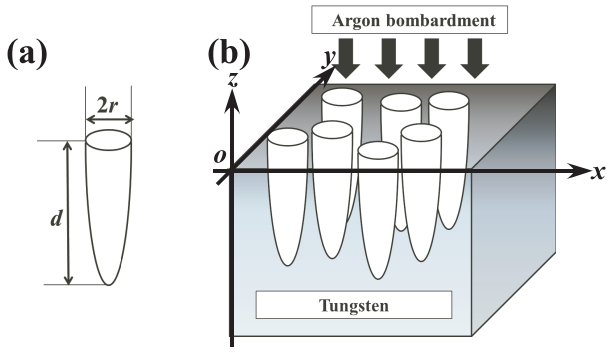

Fig. 1 Initial conditions of the tungsten target. N = 10, 20, 30, 40, or 50 half-spheroids were hollowed from the flat BCC tungsten surface (100). (a) The equatorial radius r of the half-spheroids was set to 5 Å, and the polar radius d was chosen from 5, 50, and 500 Å. (b) An argon atom with 100 eV was injected into this tungsten target. The *o-xyz* coordinate system is used in the simulation.

2. Simulation

2.1 AC∀T simulation

To evaluate the sputtering yield for Ar irradiation onto tungsten, we used the AC∀T code. In the AC∀T code [16], BCA is adopted to simulate a two-body interaction between a projectile and a target atom. The final position and velocity of the projectile and the target atom were calculated analytically using the Moliere approximation [20–22] with the following Thomas-Fermi potential $V(r)$:

$$V(r) = \frac{Z_1 Z_2 e^2}{r} \Phi\left(\frac{r}{a}\right), \tag{1}$$

where r is the distance between the projectile and the target atom, a is the screen length, and Z_1 and Z_2 are the atomic numbers of the projectile and the target atom, re-

author's e-mail: hnakamura@nifs.ac.jp

*) This article is based on the presentation at the 25th International Toki Conference (ITC25).

spectively. The following equation of the normalized distance X was adopted in AC∀T [22] as the screening potential Φ in Eq. (1):

$$\Phi(X) = 0.35e^{-0.3X} + 0.55e^{-1.2X} + 0.10e^{-6.0X}. \quad (2)$$

2.2 Tungsten target model

In the AC∀T code, we adopted a body-centered cubic (BCC) crystal with a (100)-surface as the tungsten target, which is 94.95 Å long, 47.25 Å wide, and 31650 Å deep. The lattice constant of tungsten is 3.165 Å. Periodic boundary conditions were imposed in the horizontal direction. All tungsten atoms were fixed to the lattice points of the BCC crystal without vibration, which means that the initial temperature of the tungsten was set to 0 K. An argon atom with a kinetic energy of 100 eV was injected vertically into the tungsten.

We simplified the fuzz tungsten structure as follows: (i) a tungsten crystal with a flat (100)-surface was prepared as the initial structure and then (ii) N = 10, 20, 30, 40, or 50 half-spheroids with equatorial radius r = 5 Å and polar radius d = 5, 50, or 500 Å were hollowed from the tungsten surface. The origins of the N half-spheroids were distributed randomly on the tungsten surface. After the tungsten target was prepared using the above method, an argon atom was injected into it from its upper side with a kinetic energy of 100 eV. The W and Ar atoms collided with each other, and then the final positions of all the atoms, *i.e.*, W and Ar, were detected in each simulation. We repeated the above simulation 200,000 times for each tungsten target with N half-spheroid-holes with a polar radius d. The initial injection position of the Ar atom was changed randomly for each simulation.

Here, we need to make two comments concerning the interactions between the projectile and the target. First, the Ar atom does not collide with other atoms inside the half-spheroids. The Ar begins interacting with the tungsten when it approaches the W atoms. Second, the surface binding energy of the fuzz was not included in our simulation.

3. Simulation Result

In the simulation of Ar irradiation onto a tungsten target, we calculated three physical quantities; sputtering yield Y, range R, and retention rate A.

The sputtering yield Y was obtained as follows. In the $N_{\rm sim}$ = 200,000 simulations of the tungsten target with N = 10, 20, 30, 40, or 50 half-spheroid holes with a polar radius d and an equatorial radius r = 5 Å, the number of tungsten atoms released from the tungsten surface were counted as $N_{\rm W}^{\rm sp}$. The sputtering yield Y is therefore $Y = N_{\rm W}^{\rm sp}/N_{\rm sim}$.

The range R is given by the following equation: $R = \sum_{i=1}^{N_{\rm sim}} |z_i^{\rm fin}|/N_{\rm sim}$, where $z_i^{\rm fin}$ is the $z-$coordinate of the final position of the irradiated Ar in the $i-$th simulation. The z = 0 plane denotes the surface of the tungsten target.

For the retention rate A, the number of the Ar atoms whose $z_i^{\rm fin} < 0$ is counted is defined as $N_{\rm Ar}^{\rm abs}$. Using these quantities, A is given by $A = N_{\rm Ar}^{\rm abs}/N_{\rm sim}$.

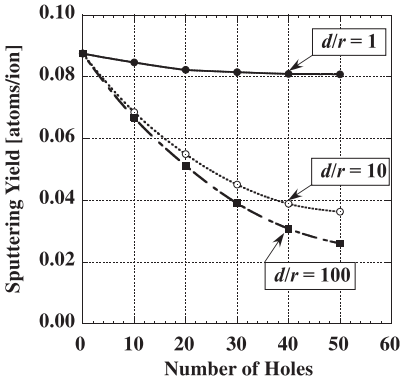

Fig. 2 Sputtering yield Y vs. the number of half-spheroid holes when the aspect ratio d/r = 1, 10, or 100 and r = 5 Å.

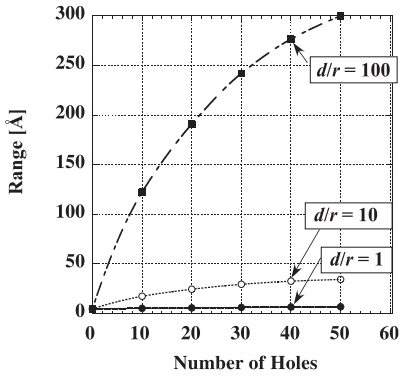

Fig. 3 Range R vs. the number of half-spheroid holes when the aspect ratio d/r = 1, 10, or 100 and r = 5 Å.

First, the number of half-spheroid holes was changed to determine the dependence on the roughness of the tungsten surface. In this case, it is expected that the number of holes corresponds to the roughness of the fuzz structure, that is, it is a flat surface when there are no holes, and as the number of holes increases the surface becomes rougher, as seen in Fig. 1. The simulation results are plotted in Figs. 2, 3, and 4 for the aspect ratios of d/r = 1, 10, and 100.

Figure 2 demonstrates that for all cases, the sputtering yield Y decreases as the number of holes increases. In addition, for all cases, the range R for all cases increases as the number of holes increases (see Fig. 3). Furthermore, Fig. 4 illustrates that the retention rate A decreases when d/r = 1 and increases when d/r = 10 and 100.

The reason why the retention rate only decreases in the case of d/r = 1 in Fig. 4 is considered as follows. In the simulation, the incident Ar atoms are injected perpendicularly onto the tungsten surface. When the surface has no holes, the Ar atom is able to easily enter the tungsten anywhere on the surface via the channeling effect. However, if there are holes (hollows) on the tungsten surface, the injection angle of the Ar atom is not perpendicular to the surfaces within the hollows. The channeling effect, there-

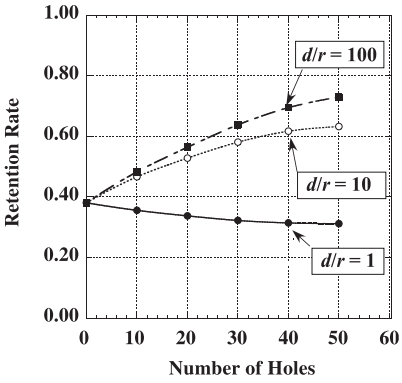

Fig. 4 Retention rate A vs. the number of half-spheroid holes when the aspect ratio d/r = 1, 10, or 100 and r = 5 Å.

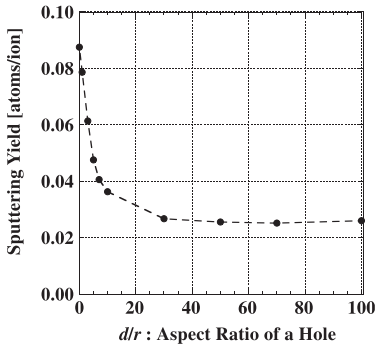

Fig. 5 Sputtering yield Y vs. the aspect ratio d/r when the number of half-spheroid holes is 50 and r = 5 Å.

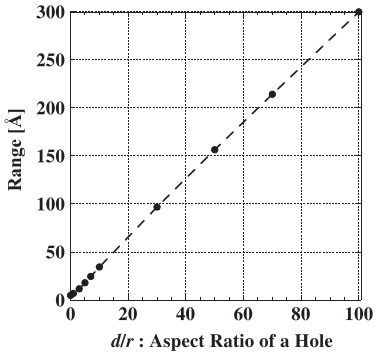

Fig. 6 Range R vs. the aspect ratio d/r when the number of half-spheroid holes is 50 and r = 5 Å.

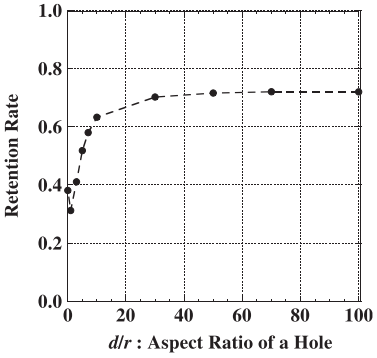

Fig. 7 Retention rate A vs. the aspect ratio d/r when the number of half-spheroid holes is 50 and r = 5 Å.

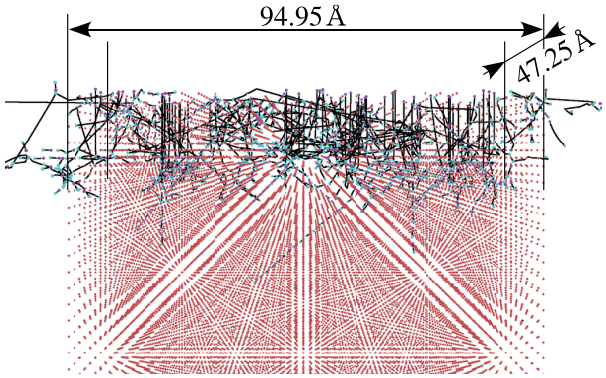

Fig. 8 (Color online) Tungsten surface irradiated by argon with d/r = 3 and r = 5 Å. The red balls denote the tungsten atoms. The purple balls denote the starting points of the moving atoms, and the blue balls denote the end point of the moving atoms. Black lines are drawn from the starting points to the end points in order to emphasize the trajectory of the moving atoms.

fore, becomes weaker, meaning that it becomes more difficult for the Ar atoms to enter the tungsten. This inference is likely correct when the depth of the hollows is not large, *i.e.*, $d/r = 1$ in Fig. 4. As the depth of the hollows increases, *i.e.*, d/r = 10 or 100 in Fig. 4, although it is difficult for the Ar atom to enter the tungsten during the first injection, the Ar atom reflected by the tungsten surface in the hollows collides with the other surfaces in the hollows. Thus, the Ar atom is captured by the hollows and the retention rate increases when d/r = 10 or 100 in Fig. 4.

Next, we investigate the influence of the thickness of the fuzz structure. The polar radius of the half-spheroid-hole d corresponds to the thickness of the fuzz structure. Therefore, we changed the aspect ratio to d/r = 0, 1, 3, 5, 7, 10, 30, 50, 70, and 100, where r = 5 Å, while the number of holes was fixed to 50. Figure 5 demonstrates that as d/r becomes larger, Y decreases and converges to $Y \sim 0.025$, which is 28 % of $Y(d/r = 0) \sim 0.087$. From Fig. 6, we find that $R \propto d/r$. Figure 7 shows that the retention rate A increases and becomes saturated at a value of $A \sim 0.73$.

To investigate the behavior of atoms, snapshots of the simulation are shown in Figs. 8 and 9. For a shallow hole, *i.e.*, d/r = 3, the irradiated Ar cannot enter the tungsten target. For a deep hole, *i.e.*, d/r = 100, the irradiated Ar can deeply penetrate the tungsten bulk.

The results of the Ar-W collision simulation demonstrate the following behavior: as the tungsten surface becomes rougher and holes becomes deeper, Ar atoms penetrate the tungsten more deeply; the invading Ar recoils against W atoms deep within the W targets; and the recoiled W has difficulty reaching the tungsten surface because the recoiled position is far from the surface.

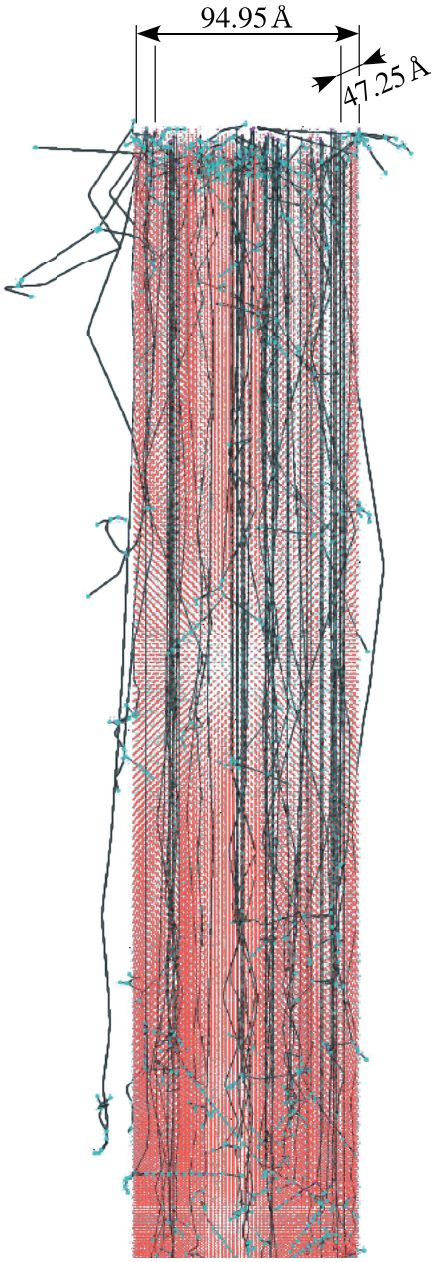

Fig. 9 (Color online) Tungsten surface irradiated by argon for d/r = 100 and r = 5 Å. The same color scheme as in Fig. 8 is used.

4. Conclusion

With the aim of investigating the reliability of the cause of reduction in the sputtering yield with fuzz suggested by Nishijima, *et al.*, we designed a half-spheroid hole model to simplify the fuzz structure and calculated the sputtering yield, the range, and the retention rate under Ar irradiation using the BCA simulation code ACAT. From the simulation, we found that the sputtering yield decreases as the depth of the holes becomes larger while the retention rate increases. This result shows that the W atoms recoiled at the bottom of the half-spheroid holes by the injected Ar atoms have difficulty escaping the W target. Therefore, we verified the reliability of Nishijima's suggestion. Moreover, because these quantities depend strongly on the surface, we assert that it is necessary to consider the surface structure of the tungsten target when estimating the effects of walls.

Acknowledgments

This work was supported by JSPS KAKENHI Grant Numbers (24656560, 26330237), MEXT KAKENHI Grant Number (25249132), and the NIFS Collaboration Research programs (NIFS14KNTS028, NIFS13KNSS-037, NIFS14KNTS030, and NIFS14KBAS016).

[1] H. Iwakiri, K. Yasunaga, K. Morishita and N. Yoshida, J. Nucl. Mater. **283-287**, 1134 (2000).
[2] D. Nishijima, M.Y. Ye, N. Ohno and S. Takamura, J. Nucl. Mater. **329-333**, 1024(2004).
[3] S. Takamura, N. Ohno, D. Nishijima and S. Kajita, Plasma Fusion Res. **1**, 051 (2006).
[4] S. Kajita, T. Saeki, Y. Hirahata, M. Yajima, H. Phno, R. Yoshihara and N. Yoshida, Jpn. J. Appl. Phys. **50**, 08JG01 (2011).
[5] S. Kajita, W. Sakaguchi, N. Ohno, N. Yoshida and T. Saeki, Nucl. Fusion **49**, 095005 (2009).
[6] S. Yajima, M. Yamagiwa, S. Kajita, N. Ohno, M. Tokitani, A. Takayama, S. Saito, A.M. Ito, H. Nakamura and N. Yoshida, J. Plasma Sci. Technol. **15**, 282 (2013).
[7] S.I. Krasheninnikov, Phys. Scr. **T145**, 014040 (2011).
[8] A.M. Ito, A. Takayama, Y. Oda, T. Tamura, R. Kobayashi, T. Hattori, S. Ogata, N. Ohno, S. Kajita, M. Yajima, Y. Noiri, Y. Yoshimoto, S. Saito, S. Takamura, T. Murashima, M. Miyamoto and H. Nakamura, J. Nucl. Mater. **463**, 109 (2015).
[9] A.M. Ito, A. Takayama, Y. Oda, T. Tamura, R. Kobayashi, T. Hattori, S. Ogata, N. Ohno, S. Kajita, M. Yajima, Y. Noiri, Y. Yoshimoto, S. Saito, S. Takamura, T. Murashima, M. Miyamoto and H. Nakamura, Nucl. Fusion **55**, 073013 (2015).
[10] D. Nishijima, M.J. Baldwin, R.P. Doerner and J.H. Yu, J. Nucl. Mater. **415**, S96 (2011).
[11] M.T. Robinson and I.M. Torrens, Phys. Rev. B **9**, 5008 (1974).
[12] J.P. Biersack and W. Eckstein, Appl. Phys. A **34**, 73 (1984).
[13] Y. Yamamura and Y. Mizuno, IPPJ-AM-40, Inst. Plasma Phys., Nagoya University, 1985, (http://dpc.nifs.ac.jp/IPPJ-AM/IPPJ-AM-40.pdf).
[14] Y. Yamamura, I. Yamada and T. Takagi, Nucl. Instrum. Methods Phys. Res. Sect. B **37-38**, 902 (1989).
[15] K. Ohya and R. Kawakami, Jpn. J. Appl. Phys. **40**, 5424 (2001).
[16] A. Takayama, S. Saito, A.M. Ito, T. Kenmotsu and H. Nakamura, Jpn. J. Appl. Phys. **50**, 01AB03 (2011).
[17] S. Saito, A. Takayama, A.M. Ito and H. Nakamura, Proc. Int. Conf. Model. Simulation Technol., 197 (2011).
[18] S. Saito, A.M. Ito, A. Takayama and H. Nakamura, J. Nucl. Mat. Suppl. **438**, S895 (2013).
[19] H. Nakamura *et al.*, ISPlasma 2014, 06aP06.
[20] M.M. Bredov, I.G. Lang and N.M. Okuneva, Zh. Tekh. Fiz. **28**, 252 (1958).
[21] M.M. Bredov, I.G. Lang and N.M. Okuneva, Sov. Phys.-Tech. Phys. **3**, 228 (1958).
[22] G. Moliere, Z. Naturforsch. **A2**, 133 (1947) (in German).